

J. M. Ugidos · K. Billström · M. I. Valladares ·
P. Barba

Geochemistry of the Upper Neoproterozoic and Lower Cambrian siliciclastic rocks and U-Pb dating on detrital zircons in the Central Iberian Zone, Spain

Received: 15 July 2002 / Accepted: 26 June 2003 / Published online: 11 September 2003
© Springer-Verlag 2003

Abstract Sandstones and shales from the Upper Neoproterozoic (UN) succession in the Central Iberian Zone (CIZ) show parallel REE patterns and relatively restricted and similar ranges and average values of some element ratios such as Al_2O_3/TiO_2 , Ti/Nb , Eu/Eu^* , $(La/Yb)_n$, $(Gd/Yb)_n$ and Th/U . This remarkable geochemical homogeneity for related medium- and fine-grained rocks is unusual, and strongly suggests a recycled source area. However, the Lower Cambrian (LC) equivalent rocks are, in general terms, geochemically less mature, more heterogeneous and more fractionated. Their average REE patterns are practically coincident, probably as a consequence of REE redistribution related to the reworking of sediments during a stage of sea level fall in Lower Cambrian times. Ti and Zr abundances, chemical index of alteration (CIA) values and element ratios such as Al_2O_3/TiO_2 , K/Rb , Ti/Nb and Rb/Zr can be used for discriminating purposes between the UN and LC siliciclastic rocks. Detrital zircons from a UN and a LC sandstone display morphological differences. However, U-Pb data are discordant and cannot be interpreted in a straightforward manner. Nevertheless, age data are compatible with a model in which the continent of Gondwana would have supplied zircons, showing a bimodal age distribution, in variable proportions to the respective sandstone units.

Keywords Geochemistry · U-Pb dating · Siliciclastics · Upper Neoproterozoic–Lower Cambrian · Iberian Massif

Introduction

In Europe pre-Mesozoic massifs show contrasting characteristics since in some cases abundant coeval volcanics are present in the Upper Neoproterozoic (UN) and Lower Cambrian (LC) sedimentary record while in other cases the volcanic contribution is lacking and the UN sediments show mature petrological and geochemical features. Examples of the former case are some areas of central-western Europe (Pin 1991 and references therein) and the Ossa Morena Zone in South Spain (Quesada et al. 1990 and references therein; Schäfer et al. 1993; Pin et al. 1999). Representative cases lacking coeval volcanics are the Central Brittany Domain (Dabard et al. 1996), the French Massif Central (Simien et al. 1999) and the Central Iberian Zone (CIZ) (Ugidos et al. 1997a, 1997b; Valladares et al. 2000, 2002a, 2002b). The Avalonian–Cadomian arc (Nance and Murphy 1994) and the North Gondwana (West Africa craton) passive continental margin (Ugidos et al. 1997a, 1997b; Valladares et al. 2000, 2002b) have been the respective geological settings suggested.

A direct comparison of Upper Neoproterozoic–Lower Cambrian sedimentary series in the CIZ and other European areas is not easy because different interpretations have been proposed, sometimes on the basis of similar petrological and geochemical results. Moreover, studies of the sedimentary series are in many cases obscured by the lack of suitable outcrops or by the effects of tectonics or metamorphism in some regions. New results in the Saxo-Thuringian areas support the notion that the Lower Cambrian sedimentary series were deposited at a passive margin on a Neoproterozoic basement overlying the Cadomian unconformity (e.g., Linnemann and Romer 2002; Kemnitz et al. 2002). This interpretation is similar to that proposed for the Lower Cambrian in the CIZ (Valladares et al. 2000). However, in the CIZ the UN–LC boundary is not an angular unconformity but, instead, a discontinuity corresponding to a sequence boundary related to a fall in sea level (Valladares et al. 2000). The Upper Neoproterozoic series in

J. M. Ugidos (✉) · M. I. Valladares · P. Barba
Departamento de Geología, Facultad de Ciencias,
Universidad de Salamanca,
37008 Salamanca, Spain
e-mail: jugidos@usal.es
Tel.: +34-923-291598
Fax: +34-923-294514

K. Billström
Swedish Museum of Natural History,
Box 50 007, 104 05 Stockholm, Sweden

Saxo-Thuringian areas are interpreted as having been deposited at an active margin (e.g., Linnemann and Romer 2002; Kemnitz et al. 2002). By contrast, a passive margin setting is the favoured interpretation for the CIZ (e.g., Beetsma 1995; Ugidos et al. 1997a, 1997b; Valladares et al. 2000, 2002a; this article). Nevertheless, a provenance from the West Africa craton is suggested for each case. A discussion challenging both interpretations on the Upper Neoproterozoic is out of the scope of this work. However, interpretations may change if the vertical evolution of geochemical features and zircon ages in the stratigraphic record can be established.

Relatively abundant U-Pb data on detrital zircons from Precambrian-Cambrian sedimentary rocks in Europe commonly define 550–600 Ma, 1.8–2.0 Ga and >2.4 Ga age intervals (Guerrot et al. 1989; Valverde-Vaquero et al. 2000; Zeh et al. 2001; Tichomirowa et al. 2001, references therein). Mainly on the basis of similar zircon ages, both the Cadomian (e.g., Guerrot et al. 1992) and the West Africa craton (e.g., Guerrot et al. 1989; Tichomirowa et al. 2001) have been proposed as sources for the Precambrian-Cambrian metasediments in some European areas. A more complex situation, with a contribution of sedimentary materials from the Avalonian-Cadomian belt, the West African and/or eastern Amazonian cratons and a minor contribution from the Grenvillian (ca. 1.0 Ga) belt, has been suggested by Zeh et al. (2001) for the protoliths of high-grade paragneisses in central European areas.

In NW Iberia, detrital zircon grains from Precambrian graywackes give U-Pb ages of 640–800 Ma, 0.9–1.2 Ga, and less abundant 1.8–2.0 Ga and Archaean ages. In the LC and Ordovician rocks ages of 640–800 Ma are almost absent and most ages are in the intervals of 550–620 Ma, 0.9–1.2 Ga, 1.8–2 Ga, a few Archaean ages also being obtained. A peri-Amazonian situation for the sedimentary basin has been proposed for NW Iberia (Fernández-Suárez et al. 2000).

As noted above, zircons of similar ages (ca. 600 Ma) are possible components of both Neoproterozoic-Cambrian sediments related to the Cadomian arc and those derived from the Pan-African orogen since in both cases igneous events developed in late Precambrian times (e.g. see Hébert 1995; Zeh et al. 2001 for Cadomian events; and e.g. Black and Liegeois 1993; Black et al. 1994 for Pan-African events). Observed detrital ages of around 0.9 to 1.0 Ga may correspond to igneous events related to an intracratonic rifting stage between 1.0 and 0.75 Ga (cf. Villeneuve and Cornée 1994), given the presence of 900–800 Ma ophiolites related to obducted crust in the northwest Africa craton (Goodwin 1991). Other evidence has been interpreted quite differently, and, for instance, relatively high ϵ_{Nd} values have been used to suggest the Avalonian-Cadomian arc as the source for the Neoproterozoic-Cambrian sediments in some European areas (e.g., Zeh et al. 2001). However, the petrological and geochemical results strongly suggest a stable continental source for Precambrian sediments, showing relatively high ϵ_{Nd} values ($\epsilon_{Nd} = -3.5$ to -0.4) in the CIZ (Beetsma

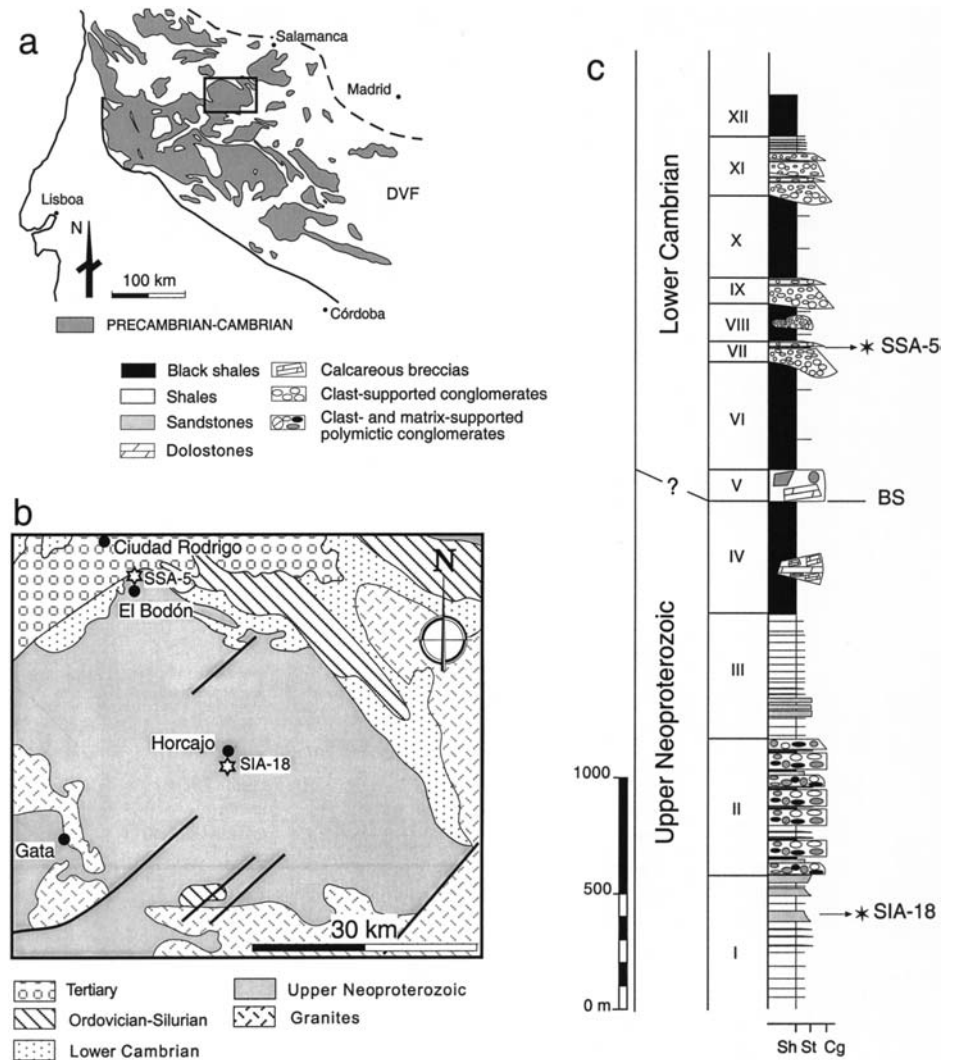
1995; Ugidos et al. 1997a, 1997b, 1999). It seems that although different geological characteristics are expected in extreme geological settings, such as a magmatic arc versus a passive setting, the latter setting has not been considered in most studies reporting zircon ages.

In the CIZ, zircon ages of sedimentary rocks have so far been lacking, but a detailed stratigraphic information on the Upper Neoproterozoic–Lower Cambrian succession is available. In the present work, we report geochemical data on UN and LC sandstones and related shales together with new U-Pb results from the conventional dating of zircons from two sandstones. The aim is to use both types of data to contribute to the discussion about the source area of the Neoproterozoic–Cambrian sedimentary materials and their evolution in SW Europe. The UN rocks strongly contrast with those from the LC since the former are geochemically mature and homogeneous, whereas those of the LC are more heterogeneous and show remarkable geochemical differences between shales and sandstones, probably related to chemical alteration and reworking of the source materials. In spite of the ambiguities related to the conventional zircon age dating of detrital zircons and possible alteration effects on U-Pb isotope systematics in the two types of rock studied, both the chemical and isotopic characteristics favour two separate source compositions, although, however, these are compatible with a common origin from north Gondwana (West Africa craton).

The Central Iberian Zone

The Iberian Massif has been divided into different zones mainly on the basis of stratigraphic and structural features (e.g., Díez Balda et al. 1990). In the Domain of Vertical Folds of the CIZ (Fig. 1a, b), extensive areas of UN and LC sediments lack coeval volcanics and significant metamorphism. In these areas, the sedimentary succession, mainly consisting of shales and sandstones, has been divided into twelve lithostratigraphic units (I to XII, Fig. 1c) organized in two depositional sequences. The total thickness ranges between 1,800 and 3,900 m. The lower sequence (units I to IV) is Upper Neoproterozoic and consists of shales and sandstones with local intercalations of matrix- and clast-supported conglomerates. The upper sequence (units V to XII) is of Early Cambrian age and its basal surface is strongly erosional and developed during an important relative sea level fall. As a result of prevailing subaerial conditions, weathering affected the materials of the Neoproterozoic–Cambrian border zone and the sediments of the uppermost Neoproterozoic units became reworked and resedimented as contributors to the Lower Cambrian units (Valladares et al. 2000, 2002a). The lowest Cambrian (unit V) consists of a megabreccia with predominantly limestone clasts at its base. Above this megabreccia there is a succession of alternations of shales (with varying abundances of organic matter and sulphides) and sandstones, with local intercalations of

Fig. 1. **a** Distribution of Upper Neoproterozoic–Lower Cambrian sedimentary rocks in the domain of vertical folds (DVF) of the Central Iberian Zone. **b** Sampling area; stars location of sandstone samples for U-Pb dating purposes. **c** Type series of the Upper Neoproterozoic–Lower Cambrian sedimentary succession in the Central Iberian Zone (after Valladares et al. 2000, simplified); *BS* boundary surface; *asterisks* positions of sandstone samples for U-Pb dating purposes



conglomerate (for a detailed description, see Valladares et al. 1998, 2000).

On the basis of geochemical, petrological and stratigraphic results most authors agree that the tectonic setting for the whole sedimentary succession has been a passive continental margin (Valladares et al. 1993, 2000, 2002a, 2002b; Beetsma 1995; Ugidos et al. 1997a, 1997b). However, the available Sm-Nd isotopic data for shales strongly support the notion that the UN series received a juvenile contribution that was greatly reduced or ceased in the LC sediments (Nägler et al. 1995; Ugidos et al. 1997b, 1999). Consequently, two main source areas have contributed to the sedimentary Upper Neoproterozoic–Lower Cambrian succession in the CIZ. Mainly from geochemical data on shales the West Africa craton and related Pan-African orogens have been suggested as the possible source areas (Ugidos et al. 1997a, 1997b; Valladares et al. 2000, 2002b).

Sampling and analytical techniques

Twenty-two samples of sandstones and shales (3–5 kg) were collected from the UN and LC sedimentary materials for analytical purposes. Coordinates of sampling points are given in Table 1. Analyses were performed using ICP-AES (major elements) and ICP-MS (all other elements) techniques at the Service d'Analyses de Roches et Minéraux of the CRPG (Nancy, France).

Two selected sandstones (25 kg) were sampled for conventional multi-grain U-Pb zircon dating: sample SIA-18 (unit I, Upper Neoproterozoic, Fig. 1) and sample SSA-5 (unit VII, Lower Cambrian, Fig. 1), about 2,500 m above the former in the stratigraphic column (Fig. 1c). The treatment of zircons at the chemistry laboratory followed standard routines, see Krogh (1973). Initially, the zircon fractions were thoroughly cleaned (with acetone in an ultrasonic bath, then with HCl and HNO₃ on a hot plate, followed by a final cleaning step with water), and finally spiked with a combined ²⁰⁵Pb/²³³–²³⁶U tracer before digestion in a HF/HNO₃ mixture. Pb and U were separated using standard ion exchange techniques

Table 1 Coordinates of sampling points

Sample	Longitude	Latitude
Lower Cambrian		
SSA-5	6°34'32"	40°30'03"
SSA-21	6°37'32"	40°28'45"
SSA-27	5°52'17"	40°37'34"
GUA-30	5°34'54"	40°38'34"
CR-2	6°39'17"	40°38'44"
SSA-18	6°37'54"	40°28'21"
SSA-19	6°39'00"	40°28'41"
SSA-24	6°03'06"	40°24'16"
SSA-25	6°10'13"	40°33'41"
CR-5	6°34'11"	40°30'44"
MIR-22	5°03'33"	40°44'45"
Upper Neoproterozoic		
SIA-11	6°07'11"	40°24'08"
SIA-18	6°21'36"	40°21'42"
SSA-11	6°14'51"	40°30'22"
SIA-26	6°29'41"	40°29'34"
FG-2	6°35'28"	40°26'23"
CPA-2	6°30'01"	40°19'15"
SIA-15	6°23'30"	40°22'50"
SIA-19	6°21'36"	40°21'42"
SIA-21	6°21'36"	40°21'42"
SIA-22	6°21'36"	40°21'42"
SIA-34	6°19'02"	40°26'36"

(HBr resin), before finally being loaded on separate Re-filaments following the silica gel-phosphoric acid loading procedure.

Pb and U aliquots were measured on a 5-collector MAT Finnigan 261 mass spectrometer, equipped with an electron multiplier, and the resulting data were plotted using the ISOPLOT/Ex, version 2.49 software package provided by Ludwig (2001).

Sandstone petrography

A detailed petrographic study of the UN and LC sandstones has been previously reported (Ugidos et al. 1997a; Valladares et al. 2000). Thus, only a brief description is given here. Certain features differ between the sandstone groups, as exemplified by the finer grain size of the UN rocks relative to those of the LC (up to 250 and 800 μm , respectively), and the lower content of albite and higher amount of fine-grained lithic components in the former rocks. The UN sandstones are lithic arenites/graywackes whereas the LC sandstones range from subfeldspathic and sublithic arenites to feldspathic, lithic and quartz wackes. According to classification schemes on the basis of the Q-L-F parameters after Dickinson et al. (1983), the UN sandstones plot in the field corresponding to a recycled orogen as the source area whereas the LC sandstones mainly plot in the field corresponding to the interior of a craton.

Geochemistry

In the present work, 11 sandstones and 11 shales from the Upper Neoproterozoic and Lower Cambrian sedimentary succession were selected for analytical work. Chemical data are presented in Tables 2 and 3.

Major elements

In general terms, the UN and LC sandstones show minor differences in average compositions and ranges of most of the oxides (Table 2 and 3) that potentially may be related to the quartz dilution effect. However, this is not the case for CaO and Na₂O contents, which are clearly lower in the UN sandstones. This probably resulted from a more intense chemical alteration of the Neoproterozoic rocks, as suggested by their higher CIA (Chemical Index of Alteration = $[\text{Al}_2\text{O}_3 / (\text{Al}_2\text{O}_3 + \text{Na}_2\text{O} + \text{K}_2\text{O} + \text{CaO}^*)] \times 100$; Nesbitt and Young 1982) values. CIA is the only parameter involving major elements that separates the two groups of sandstones.

Both groups of shales also show similar average compositions and ranges and reflect chemical features that are comparable to those in the corresponding sandstones, such as lower CaO and Na₂O contents and higher CIA values of the UN shales. However, other parameters such as the TiO₂ contents and Al₂O₃/TiO₂ ratios clearly separate the UN from the LC shales (Fig. 2a).

Both the shales and sandstones show negative SiO₂-major element correlations for TiO₂, Al₂O₃, K₂O, and Fe₂O₃ but only Al₂O₃-TiO₂ and Al₂O₃-K₂O covariations (diagrams not included) are well defined in the sandstones and absent or poorly defined in the shales. This latter aspect is probably a consequence of the relatively narrow range of the Al₂O₃ content in the shales.

Trace elements

Rb, Sr, Ba, Th, U

With the exception of the relatively higher Sr content in the LC sandstones, the ranges of contents of all the other elements partially overlap. However, the UN sandstones have relatively more restricted ranges of element abundances (see Tables 2 and 3) than those of the LC.

The shales show features similar to those of the corresponding sandstones, i.e. overlapping ranges of the respective abundances of the same elements and the very narrow ranges of some element abundances (e.g., Rb, Ba, Th). The K-Rb and K-Ba plots (Fig. 2b, c) show good positive correlations (except for Ba in some LC sandstones) and point to a change in the covariation slopes of the UN shales with respect to the corresponding sandstones. These changes in the slopes are probably due to some differences in the relative abundances of K-rich minerals, although some mobility of Rb and Ba should

Table 2 Chemical data of Upper Neoproterozoic shales and sandstones from the CIZ

Sample	SIA-11	SIA-18	SSA-11	SIA-26	FG-2	CPA-2	Avg.	SIA-15	SIA-19	SIA-21	SIA-22	SIA-34	Avg.
SiO ₂	72.05	71.31	69.77	73.81	75.49	77.7	73.36	59.64	60.11	58.48	57.17	60.79	59.24
TiO ₂	0.71	0.76	0.76	0.73	0.53	0.57	0.68	1.04	1.07	1.09	1.07	1.00	1.05
Al ₂ O ₃	13.13	13.72	13.27	12.16	10.91	9.20	12.07	19.51	19.91	19.96	20.37	19.84	19.92
Fe ₂ O ₃	5.01	4.98	6.78	5.29	4.51	5.34	5.32	6.91	5.85	7.14	7.91	7.15	6.99
MgO	1.86	1.56	1.96	1.41	1.52	1.81	1.69	2.54	2.07	2.50	2.70	2.25	2.41
MnO	-	0.03	0.04	0.04	0.05	0.05	0.04	0.02	0.02	0.04	0.04	0.04	0.03
CaO	0.05	0.50	0.63	0.49	0.58	0.61	0.48	0.19	0.12	0.12	-	0.05	0.12
Na ₂ O	1.60	2.04	1.71	1.71	2.09	0.49	1.61	1.19	1.37	1.54	1.12	1.44	1.33
K ₂ O	2.19	2.35	1.89	1.89	1.59	1.20	1.85	3.95	4.66	4.17	4.17	3.59	4.11
P ₂ O ₅	0.14	0.15	0.30	0.09	0.11	0.17	0.16	0.26	0.23	0.25	0.26	0.19	0.24
LOI	3.03	2.33	2.67	2.12	2.46	2.67	2.55	4.47	4.27	4.34	4.93	3.45	4.29
Total	99.78	99.73	99.78	99.74	99.84	99.81	99.78	99.72	99.68	99.63	99.74	99.79	99.71
Rb	85	85	69	70	59	45	69	133	142	136	134	133	136
Sr	59	87	67	78	95	64	75	57	44	57	43	100	60
Ba	402	479	333	373	290	223	350	783	846	824	804	744	800
La	32.84	30.80	31.68	31.50	21.69	30.23	29.79	46.39	54.02	46.47	33.05	44.75	44.94
Ce	73.10	67.26	70.94	74.08	44.75	75.13	67.54	98.49	110.90	96.60	69.23	90.63	93.17
Pr	7.89	7.64	8.06	7.92	5.00	7.28	7.30	11.62	13.45	11.98	8.93	11.12	11.42
Nd	30.52	29.62	32.01	28.81	19.86	28.84	28.28	45.95	55.91	47.38	36.58	44.15	45.99
Sm	5.91	5.72	7.34	6.07	4.61	6.06	5.95	9.42	11.54	10.03	7.56	8.63	9.44
Eu	1.28	1.23	1.53	1.33	0.96	1.19	1.25	2.12	2.13	1.93	1.61	1.83	1.92
Gd	4.87	4.29	6.78	5.03	4.02	5.33	5.05	7.81	9.30	8.25	6.51	6.68	7.71
Tb	0.77	0.65	1.21	0.81	0.59	0.77	0.80	1.23	1.34	1.29	1.03	1.00	1.18
Dy	4.42	4.06	7.07	4.61	3.28	4.61	4.68	7.88	8.13	7.57	6.36	5.91	7.17
Ho	1.00	0.91	1.46	0.90	0.68	1.04	1.00	1.71	1.84	1.71	1.50	1.19	1.59
Er	2.50	2.52	3.69	2.46	1.93	2.69	2.63	4.31	4.71	4.23	3.90	3.14	4.06
Tm	0.36	0.39	0.52	0.39	0.29	0.42	0.40	0.64	0.70	0.65	0.61	0.53	0.63
Yb	2.52	2.63	3.39	2.44	2.06	2.59	2.61	4.18	4.64	4.29	3.84	3.40	4.07
Lu	0.41	0.40	0.46	0.41	0.34	0.34	0.39	0.64	0.66	0.64	0.57	0.52	0.61
Eu/Eu*	0.73	0.76	0.66	0.74	0.68	0.64	0.70	0.76	0.63	0.65	0.70	0.74	0.70
(La/Yb) _n	8.81	7.91	6.31	8.72	7.12	7.89	7.79	7.50	7.87	7.32	5.82	8.89	7.48
(Gd/Yb) _n	1.57	1.32	1.62	1.67	1.58	1.67	1.57	1.51	1.62	1.56	1.37	1.59	1.53
∑REE	168	158	176	167	167	110	158	242	279	243	181	223	234
Y	24	22	41	27	19	28	27	39	46	40	38	32	39
Zr	273	293	250	306	209	248	263	245	287	247	238	247	253
Hf	7.2	8.3	6.2	7.6	5.5	6.3	6.8	7.4	8.1	7.1	6.8	6.7	7.2
Th	10.1	11.0	9.8	9.3	8.0	8.9	9.5	14.0	14.5	14.3	14.2	11.7	13.8
U	2.9	3.1	2.9	2.6	2.1	2.3	2.7	3.9	4.3	4.3	4.2	3.4	4.0
V	93	92	77	73	65	58	76	141	146	152	150	126	143
Nb	10	11	10	10	7	9	10	14	15	15	15	14	15
Cr	83	93	80	79	68	67	78	120	129	130	128	117	125
Co	38	29	27	27	27	30	30	15	17	12	15	11	14
Ni	27	40	40	29	27	16	30	27	33	27	28	38	31
Pb	24	24	26	16	16	36	24	16	15	18	22	13	17
Al ₂ O ₃ /TiO ₂	18.5	18.1	17.5	16.1	16.7	20.6	17.9	18.8	18.6	18.3	19.0	19.8	18.9
CIA	73.4	68.0	71.5	68.7	67.9	76.6	71.0	76.6	74.0	74.9	78.0	77.1	76.1
K/Rb	214	230	227	224	224	221	223	247	272	255	258	224	251
Ti/Zr	15.6	15.6	18.2	14.3	15.2	13.8	15.4	25.5	22.4	26.5	27.0	24.3	25.1
Ti/Nb	417	422	437	429	442	387	422	433	419	424	417	423	423
Rb/Zr	0.31	0.29	0.28	0.23	0.28	0.18	0.26	0.54	0.49	0.55	0.56	0.54	0.54
Zr/Hf	37.9	35.5	40.7	40.3	38.2	39.6	38.7	33.0	35.3	34.9	35.3	36.9	35.1
Th/Yb	4.01	4.18	2.90	3.83	3.86	3.43	3.70	3.35	3.13	3.33	3.70	3.45	3.39
Th/U	3.4	3.5	3.4	3.8	3.6	3.8	3.6	3.6	3.4	3.4	3.4	3.5	3.4

not be ruled out. A remarkable distinctive feature is the Th-U positive covariation (Fig. 2d) defined by the UN rocks, which is absent in the LC rocks.

The K/Rb ratio values are higher in the UN than in the LC shales (224 to 258 and 182 to 211, respectively) and a similar difference is also recorded for all but one corresponding sandstones. Thus, the K/Rb ratio is a good parameter to separate the UN from LC rocks, although it should not be used exclusively. Th/U ratios range between 3.4–3.8 in the Neoproterozoic shales but show a wider range (2.3–5.9) in the Lower Cambrian ones. These Th/U values are comparable to that recorded for the upper continental crust (average Th/U=3.8; Taylor and McLennan 1985).

Rare earth elements (REE), Y

The average REE pattern (Fig. 3) of the UN sandstones shows a lower average chondrite-normalized value of light rare earth elements (LREE) than the LC sandstones but the patterns for the heavy rare earth elements (HREE) are the same. The former rocks are less fractionated, as is indicated by their higher Eu/Eu* (0.64 to 0.76) and lower (La/Yb)_n (6.31 to 8.72) and Th/Yb (2.9 to 4.18) ratios than the LC ones (0.57 to 0.72, 7.75 to 12.29 and 3.39 to 7.94, respectively).

Both groups of shales show similar REE patterns (Fig. 3) but the UN ones are relatively more enriched in the whole REE. The Eu/Eu* ratios are also similar (0.63

Table 3 Chemical data of Lower Cambrian shales and sandstones from the CIZ

Sample	SSA-5	SSA-21	SSA-27	GUA-30	CR-2	Avg.	SSA-18	SSA-19	SSA-24	SSA-25	CR-5	MIR-22	Avg.
SiO ₂	71.93	74.11	63.92	78.51	63.78	70.45	56.09	62.60	57.73	57.45	58.71	59.34	58.65
TiO ₂	0.67	0.64	0.71	0.49	0.75	0.65	0.61	0.66	0.76	0.72	0.75	0.82	0.72
Al ₂ O ₃	11.33	11.31	16.81	10.32	16.22	13.20	18.19	14.08	20.91	18.16	19.11	19.19	18.27
Fe ₂ O ₃	6.29	4.00	6.30	2.21	6.37	5.03	7.94	6.12	7.00	6.32	7.27	6.98	6.94
MgO	1.78	1.87	2.48	0.67	3.15	1.99	2.20	3.70	2.59	2.49	3.30	2.93	2.87
MnO	0.12	0.08	0.08	0.02	0.21	0.10	0.03	0.07	0.04	0.04	0.10	0.08	0.06
CaO	1.32	0.91	0.99	1.35	1.10	1.13	0.67	1.59	0.15	0.03	0.50	0.85	0.63
Na ₂ O	3.27	2.97	2.46	3.12	1.99	2.76	1.46	1.32	1.48	1.20	2.04	2.17	1.61
K ₂ O	0.57	1.25	2.91	1.60	2.74	1.81	3.56	2.16	4.10	3.80	3.48	3.33	3.41
P ₂ O ₅	0.16	0.14	0.18	0.13	0.16	0.15	0.15	0.98	0.14	0.11	0.20	0.14	0.29
LOI	2.37	2.50	2.71	1.45	3.23	2.45	8.79	6.45	4.80	8.95	4.27	3.17	6.07
Total	99.81	99.78	99.55	99.87	99.70	99.74	99.69	99.73	99.70	99.77	99.73	99.00	99.60
Rb	23	51	143	73	79	74	162	94	184	157	137	143	146
Sr	142	78	162	264	152	160	105	66	82	91	68	187	100
Ba	99	282	609	392	653	407	894	418	749	1486	618	567	789
La	34.38	31.88	47.83	37.84	34.39	37.26	22.41	35.23	44.60	40.34	36.77	47.15	37.75
Ce	79.23	68.08	91.27	77.46	73.45	77.90	44.28	72.27	90.16	74.96	73.22	87.78	73.78
Pr	8.28	7.85	10.76	8.91	8.45	8.85	5.46	8.91	10.95	9.10	8.90	10.70	9.00
Nd	31.81	29.80	40.28	33.73	61.41	33.41	21.16	34.06	43.01	35.40	34.90	39.19	34.62
Sm	6.31	6.20	8.32	5.94	6.77	6.71	4.33	8.04	8.32	6.93	6.76	7.58	6.99
Eu	1.04	1.25	1.69	0.96	1.33	1.25	1.03	1.60	1.85	1.40	1.45	1.57	1.48
Gd	4.96	5.26	6.19	4.63	5.58	5.32	3.80	8.76	6.64	5.03	5.62	6.01	5.98
Tb	0.78	0.82	0.93	0.67	0.90	0.82	0.59	1.27	0.97	0.77	0.85	0.96	0.90
Dy	4.62	4.78	5.57	3.80	5.13	4.78	3.73	8.10	5.64	4.70	4.85	5.43	5.41
Ho	0.92	0.98	1.03	0.73	1.10	0.95	0.75	1.60	1.11	0.87	1.09	1.04	1.08
Er	2.38	2.60	2.90	1.94	2.99	2.56	2.35	4.42	3.26	2.30	2.89	2.79	3.00
Tm	0.33	0.39	0.41	0.31	0.46	0.38	0.37	0.70	0.48	0.35	0.43	0.41	0.46
Yb	2.34	2.51	2.77	2.08	3.00	2.54	2.56	4.55	3.20	2.79	3.02	2.72	3.14
Lu	0.36	0.38	0.41	0.32	0.52	0.40	0.42	0.68	0.49	0.40	0.40	0.42	0.47
Eu/Eu*	0.57	0.67	0.72	0.56	0.66	0.64	0.78	0.58	0.76	0.72	0.72	0.71	0.71
(La/Yb) _n	9.93	8.58	11.67	12.29	7.75	10.04	5.92	5.23	9.42	9.77	8.23	11.73	8.38
(Gd/Yb) _n	1.72	1.70	1.81	1.80	1.51	1.71	1.20	1.56	1.68	1.46	1.51	1.79	1.53
∑REE	178	163	220	179	175	183	113	190	221	185	181	214	184
Y	25	28	31	21	30	27	23	51	36	24	29	29	32
Zr	289	237	195	355	156	246	125	194	174	150	149	147	157
Hf	7.0	6.6	5.2	9.3	4.3	6.5	3.3	4.5	4.5	4.1	4.2	4.0	4.1
Th	10.2	9.1	12.0	16.5	10.2	11.6	11.4	8.8	12.3	14.4	10.9	17.9	12.6
U	2.8	2.7	3.0	2.8	3.3	2.9	3.8	3.3	2.8	6.2	3.0	3.2	3.7
V	63	62	95	33	122	75	124	110	128	139	112	112	121
Nb	8	9	13	10	11	10	10	11	13	13	11	15	12
Cr	67	54	82	32	93	66	90	80	111	93	100	103	96
Co	47	29	25	47	32	36	32	28	13	113	23	20	38
Ni	33	27	43	12	59	35	82	61	45	100	50	50	65
Pb	19	15	19	19	18	18	37	28	11	38	15	36	28
Al ₂ O ₃ /TiO ₂	16.9	17.7	23.7	21.1	21.6	20.2	29.8	21.3	27.5	25.2	25.5	23.4	25.5
CIA	58.5	59.9	66.2	53.4	67.3	61.1	71.8	73.5	75.4	75.5	71.6	69.6	72.9
K/Rb	206	203	169	183	288	210	182	191	185	201	211	193	194
Ti/Zr	13.9	16.2	21.8	8.3	28.8	17.8	29.3	20.4	26.2	28.8	30.2	33.4	28.0
Ti/Nb	490	413	318	303	418	389	359	361	338	330	394	331	352
Rb/Zr	0.08	0.22	0.73	0.20	0.51	0.35	1.30	0.48	1.06	1.05	0.92	0.97	0.96
Zr/Hf	41.1	35.8	37.6	38.2	36.6	37.9	38.3	43.0	38.9	37.0	35.2	37.1	38.3
Th/Yb	4.36	3.64	4.34	7.94	3.39	4.73	4.45	1.94	3.83	5.16	3.61	6.60	4.27
Th/U	3.6	3.5	4.1	5.9	3.1	4.0	3.0	2.6	4.4	2.3	3.6	5.6	3.6

to 0.76 and 0.58 to 0.78) but the ranges of the (La/Yb)_n and Th/Yb ratios are wider in the LC (5.23 to 11.73 and 1.94 to 6.60) than in the UN shales (5.82 to 8.89 and 3.13 to 3.70). This is also the case for the corresponding sandstones (see above). The LC rocks also have the highest values of these two latter parameters.

The average REE patterns of the UN shales and sandstones are parallel (Fig. 3) and the former are more REE-enriched than the sandstones. This is the normal case, i.e., the REE abundances in sandstones are generally lower than in shales if no mineral fractionation has affected the sediments (e.g., Taylor and McLennan 1985; McLennan 1989; Bock et al. 1994; Cullers 1995). As a consequence, both groups of rocks present similar rele-

vant trace element ratios such as (La/Yb)_n, Zr/Yb, etc. Thus, the data suggest that the fractionation of REE-bearing minerals did not affect the UN detritus along with sedimentary processes. However, for the LC succession both the shales and the sandstones have similar average REE patterns and only minor differences in Eu and HREE (Fig. 3). In fact both rock types have very similar average REE contents. This is an uncommon feature, probably related to some REE redistribution in the LC sediments that led shales and sandstones to acquire similar whole REE abundances. The possible cause for this redistribution is considered below. The Y abundances are slightly higher in both groups of shales relative to the corresponding groups of sandstones but there are no significant

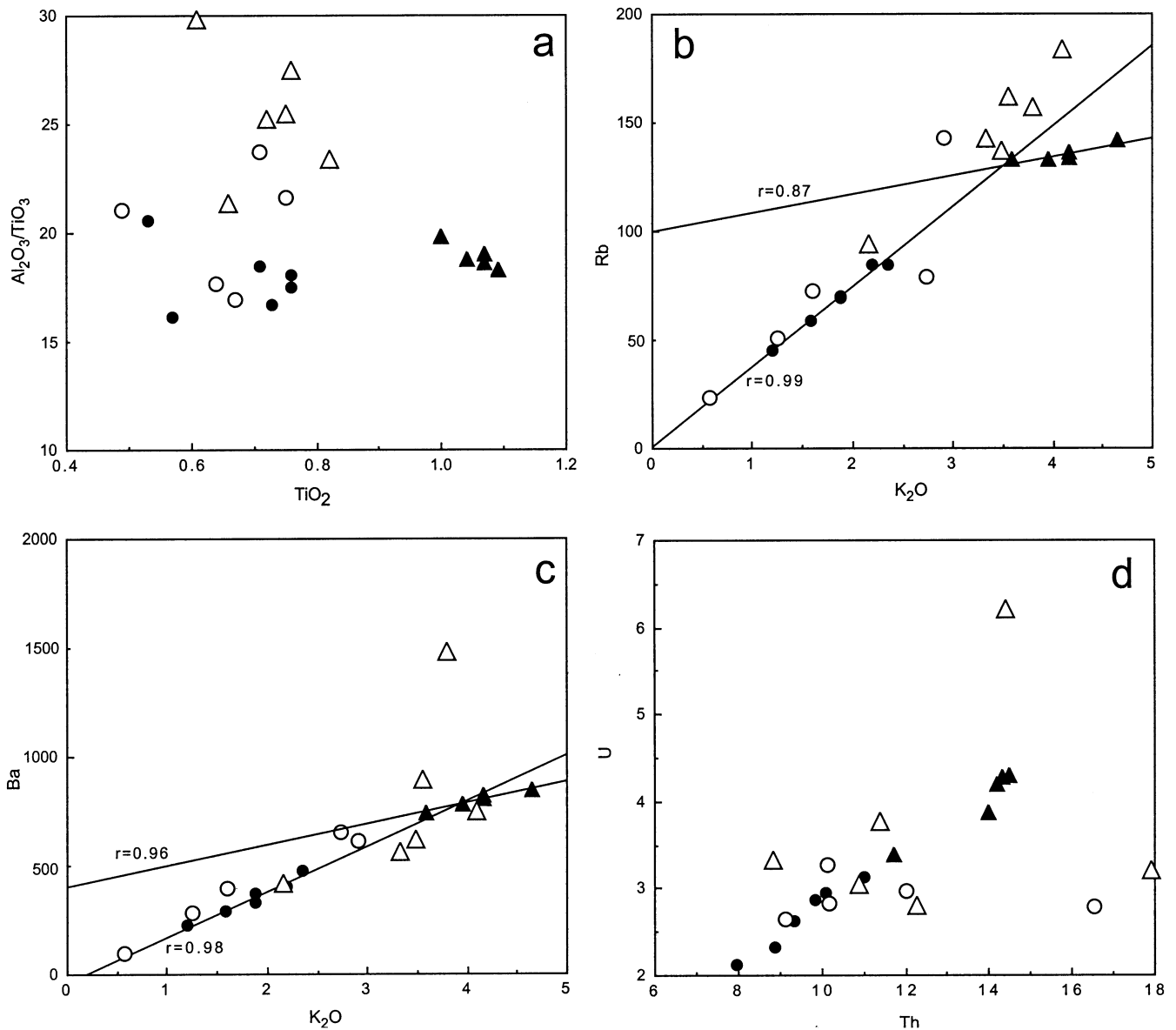


Fig. 2a–d Selected major and trace element diagrams of the Upper Neoproterozoic and Lower Cambrian siliciclastic rocks. *Filled* and *open circles* Upper Neoproterozoic and Lower Cambrian sandstones, respectively. *Filled* and *open triangles* Corresponding

shales. Note the different fields defined by the shales (a), the slopes of the K_2O -Rb and K_2O -Ba plots of the Upper Neoproterozoic shales (b, c) and the positive Th-U covariation (d) for the Upper Neoproterozoic rocks

differences between the UN and LC rocks. Y abundances and ratios involving this element mimic those of the HREE in all groups.

Zr, Hf, Nb

Both groups of sandstones show similar average contents of Zr, Hf and Nb but, as in the case of other elements, the LC sandstones show wider ranges of contents of these elements than do the UN rocks. Similarly, the Zr/Hf, Ti/Zr and Ti/Nb ratios also show wider ranges of values in the LC rocks. As a consequence the values of all these parameters overlap strongly.

The UN shales show higher and more restricted ranges of Zr, Hf and Nb contents than the LC rocks. The range of Ti/Zr ratios in the UN shales is restricted (22.35 to 26.95) but rather wide in the LC shales (20.40 to 33.36). This is also the case of the Ti/Nb ratio, which moreover is a good discriminating parameter between both groups of shales since the ranges of values do not overlap (see Table 2 and 3). Other distinctive features are that the UN sandstones and shales show similar Zr abundances and Ti/Nb ratios whereas Zr content in the LC sandstones is higher than in the corresponding shales. The Rb/Zr ratio also shows a lower and very restricted range of values in the UN rocks. This parameter can be used as a good discriminant for the two groups of shales, given the remarkable difference

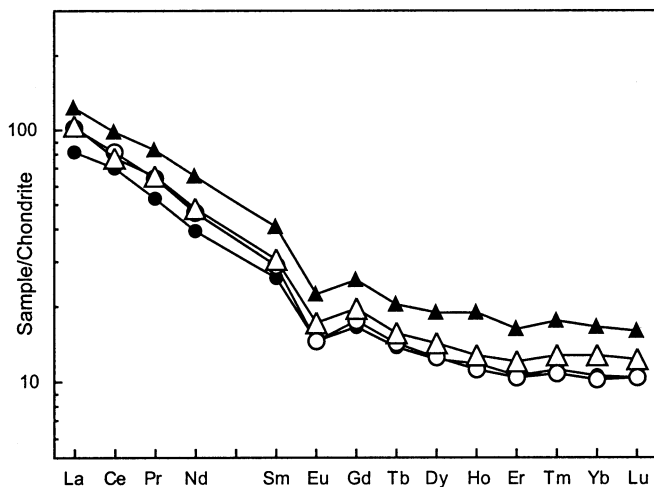


Fig. 3 Average REE patterns of the shales and sandstones studied. Symbols as in Fig. 2. Normalizing chondrite values after Taylor and McLennan (1985)

between their ranges and average values (see Tables 2 and 3).

The Zr-HREE diagram (Fig. 4a) shows a positive covariation for the LC shales and a negative one for the corresponding sandstones. Given that zircon is a HREE carrier, these covariations are difficult to explain in terms of a simple process of mineral sorting since in this case the Zr-HREE covariations should be positive, or lacking if more HREE-bearing minerals were present in significant abundances. Moreover, the Zr content in the LC sandstones is higher than in the corresponding shales (Fig. 4a, Table 3) and a positive Zr-HREE covariation, rather than a negative one, would be the expected feature. Therefore, such covariations suggest a more complex process than simple fractionation of HREE in shales with respect to sandstones. Additionally, the (La/Yb)_n ratio has a relatively wide range of values for practically constant Zr abundances of around 150 ppm (Fig. 4b). Thus, an LREE-bearing mineral phase must have controlled this ratio. Possibly, a combination of REE mobilization and mineral fractionation would have caused the observed REE distribution. A study of the REE-bearing mineral phases or specific alteration processes is, however, out of the scope of this work. Nevertheless, it has been indicated that under different circumstances, including those related to weathering (e.g., Nesbitt 1979; Nesbitt and Wilson 1992; Cotten et al. 1995), REE elements are mobile. It is also known that soil horizons may be depleted in some REE while others are enriched in such elements (e.g., Nesbitt and Markovicks 1997; Öhlander et al. 2000). Thus, it is suggested that HREE fractionation in the fine-grained materials would have resulted from the subaerial reworking of the uppermost Neoproterozoic sediments (see above).

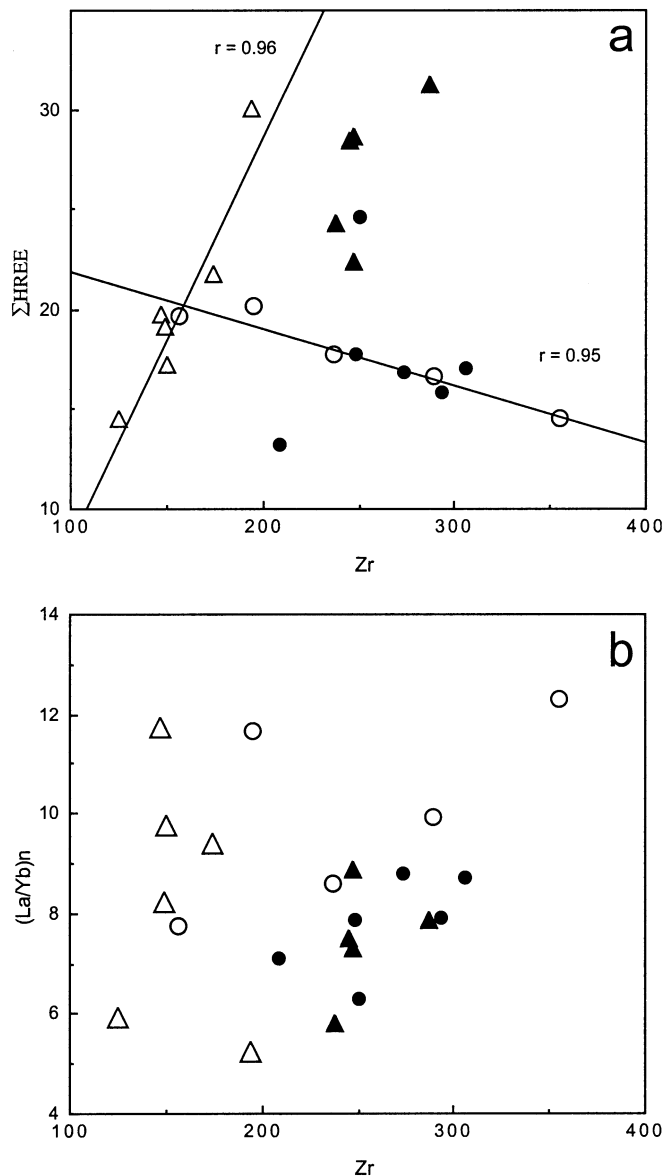


Fig. 4. a Zr-HREE diagram: *negative* and *positive* covariations for the Lower Cambrian sandstones and shales, respectively. By contrast, the Upper Neoproterozoic rocks lack these covariations. **b** Zr-(La/Yb)_n diagram. Broad range of (La/Yb)_n ratios in the Lower Cambrian shales for a relatively narrow range of Zr contents. See text. Symbols as in Fig. 2

Cr, V, Co, Ni

Cr abundances are slightly higher in the UN rocks than in the corresponding LC ones for the same Al₂O₃ contents, although V contents are similar. These elements show positive covariation (diagrams not included) with Al₂O₃, probably because they are adsorbed by clays and there are no other V or Cr minerals. Co and Ni abundances are variable and show a more restricted range of contents in the UN than in the LC rocks. Comparisons are not possible on the basis of whole rock analyses of these

Table 4 U-Pb zircon data for the investigated samples from the Central Iberian Zone, Spain

Sample	Weight (mg)	Conc. (ppm)		$^{206}\text{Pb}/^{204}\text{Pb}$ (meas.)	Radiogenic Pb (at%)		Atomic ratios		Apparent ages (Ma)							
		U	Pb _{tot}		$^{206}\text{Pb}/^{207}\text{Pb}$	$^{208}\text{Pb}/^{207}\text{Pb}$	$^{206}\text{Pb}/^{238}\text{U}$	Error±	$^{207}\text{Pb}/^{235}\text{U}$	Error±	$^{206}\text{Pb}/^{238}\text{U}$	$^{207}\text{Pb}/^{235}\text{U}$	$^{207}\text{Pb}/^{206}\text{Pb}$			
SSA-5 sandstone																
A, Fragmented	0.0151	353	53	1,271	78.7	7.9	13.4	0.1363	10	1.730	15	0.0920	04	824	1,020	1,468
B, Rounded	0.0068	1,615	101	524	78.3	7.1	14.6	0.0350	10	0.3338	112	0.0692	10	222	292	905
C, Prismatic	0.0116	507	52	466	77.9	6.9	15.2	0.0893	09	0.7486	99	0.0608	05	551	567	632
D, Fragmented, metamict	0.0057	2,038	221	218	72.1	9.2	18.7	0.0838	08	0.7142	93	0.0618	05	518	547	669
SIA-18 sandstone																
E, Fragmented	0.0242	397	55	1,675	76.7	6.6	16.7	0.1219	07	1.3385	101	0.0797	04	741	863	1,189
F, Rounded, multi-faceted	0.0264	120	13	506	75.3	6.1	18.6	0.0948	06	0.7879	136	0.0603	10	584	590	613
G, Euhedral, yellow	0.0346	376	43	4,762	82.4	5.9	11.7	0.1095	08	1.0575	92	0.0700	03	670	733	929
H, Euhedral, pink	0.0308	411	64	5,873	83.2	7.8	9.0	0.1490	14	1.9032	186	0.0926	02	895	1,082	1,480
I; Pink balls	0.104	282	79	4,108	78.7	10.4	10.9	0.2545	21	4.5366	370	0.1293	01	1,462	1,738	2,088
2, Oval-shaped, rounded	0.101	318	46	3,263	81.7	8.4	9.9	0.1367	09	1.8766	128	0.0995	02	826	1,073	1,615
3, Rounded, multi-faceted	0.0971	306	34	3,506	83.3	5.9	10.8	0.1069	12	0.9868	114	0.0669	02	655	697	835
4, Euhedral, colourless	0.0556	479	59	4,151	83.6	6.3	10.1	0.1192	15	1.1860	159	0.0721	03	726	794	990
5, Fragmented	0.0476	415	69	6,055	79.0	8.2	12.8	0.1535	13	2.1708	184	0.1025	02	921	1,172	1,671

$^{206}\text{Pb}/^{204}\text{Pb}$ corrected for mass discrimination only, all other atomic ratios corrected also for blank and initial lead. Errors are given at least significant digits at the 95% confidence level. Discrimination Pb 0.12% / AMU, U 0.05% / AMU. Blank levels; Pb: ca.10 pg, U: ca. 3 pg.

elements because of the relative abundance of sulphides in the LC shales.

U-Pb results

Perhaps the most outstanding feature of the U-Pb zircon data (Table 4) is the fact that most analyses plot in a very discordant manner (Figs. 5 and 6). This feature complicates the interpretation of data, since several explanations can be put forward to assess the history of a specific zircon population. Moreover, discordant data deriving from multi-grain fractions are even more ambiguous to interpret, since discrete grains within the selected population may have had different geological histories. The rocks sampled are sediments that may hypothetically be composed of detritus from several source areas involving bedrocks of different ages. As a first approximation the $^{207}\text{Pb}/^{206}\text{Pb}$ ages may be used to group the zircon data obtained. It should be noted, however, that in a U-Pb system that has suffered post-crystallization disturbances, such ages for discordant data points are minimum ages and may have no geological meaning.

For the SSA-5 sample, data exist from four different, but morphologically rather similar, zircon fractions (Fig. 5). Two of these, i.e. C (subhedral to euhedral grains) and D (subhedral and somewhat turbid crystals) are moderately discordant and indicate $^{207}\text{Pb}/^{206}\text{Pb}$ ages close to 0.7–0.6 Ga. The slightly rounded grains, defining fraction B, plot more discordantly and the $^{207}\text{Pb}/^{206}\text{Pb}$ ratio for this fraction sets a minimum age limit at 905 Ma.

Finally, fraction A (more angular, fragmented grains) appears to indicate an older history. Its $^{207}\text{Pb}/^{206}\text{Pb}$ ratio suggests a formation prior to 1.47 Ga.

A larger U-Pb isotope data set is available for the SIA-18 sample and a complex pattern emerges when data are plotted (Fig. 6). The fraction F, which corresponds to a multi-faceted zircon type, is nearly concordant and appears to be significantly younger than the other fractions in the sense that it indicates a formation close to 0.6 Ga. Of the remaining fractions, #3, 4 and G are highly discordant and have relatively low $^{207}\text{Pb}/^{206}\text{Pb}$ ages: between 0.8–1.0 Ga. It is also evident, however, that certain trends for linear relationships appear. For instance, fractions #3, 5, E and G tentatively form a semi-linear arrangement in Fig. 6. If this linear relationship were significant, it would suggest that the corresponding zircon fractions stem from sources of roughly the same age (upper intersection with concordia) in the 1.7 to 1.8 Ga interval, and the inferred lower intersection could also mark a common Pb-loss event at ca. 0.6 Ga. The remaining fractions indicate source ages that are definitely older than 1.0 Ga and if, analogous to the above process, an episodic Pb-loss at 0.6 Ga is relevant then the resulting source ages would exceed 2.0 Ga. Irrespective of hypothetical Pb losses linked to post-crystallization events, a clear indication of a provenance age older than 2.0 Ga is provided by fraction 1. Zircons of this fraction, which appear as rounded, almost ball-shaped crystals, must have formed prior to 2.0 Ga.

Fig. 5 U-Pb concordia of the Lower Cambrian SSA-5 sandstone sample. Also shown is the effect of a tentative two-stage, post-crystallization episodic Pb-loss event on the zircon U-Pb systematics (the data plot inside a triangle-shaped area) assuming the source rock area to have a restricted age with a mean of 2.0 Ga

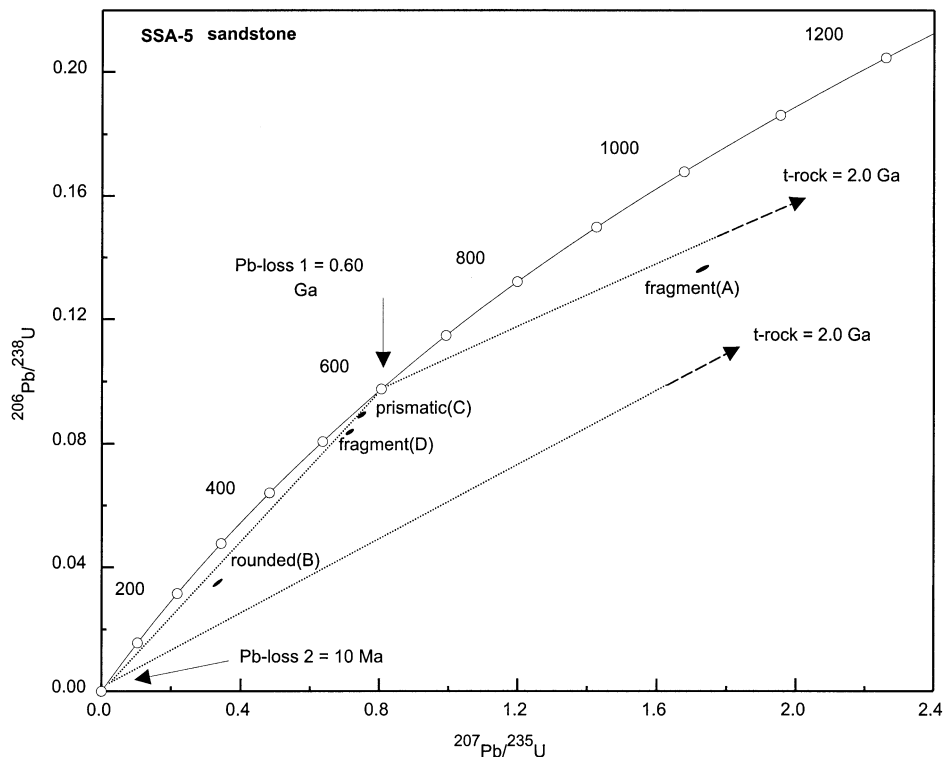
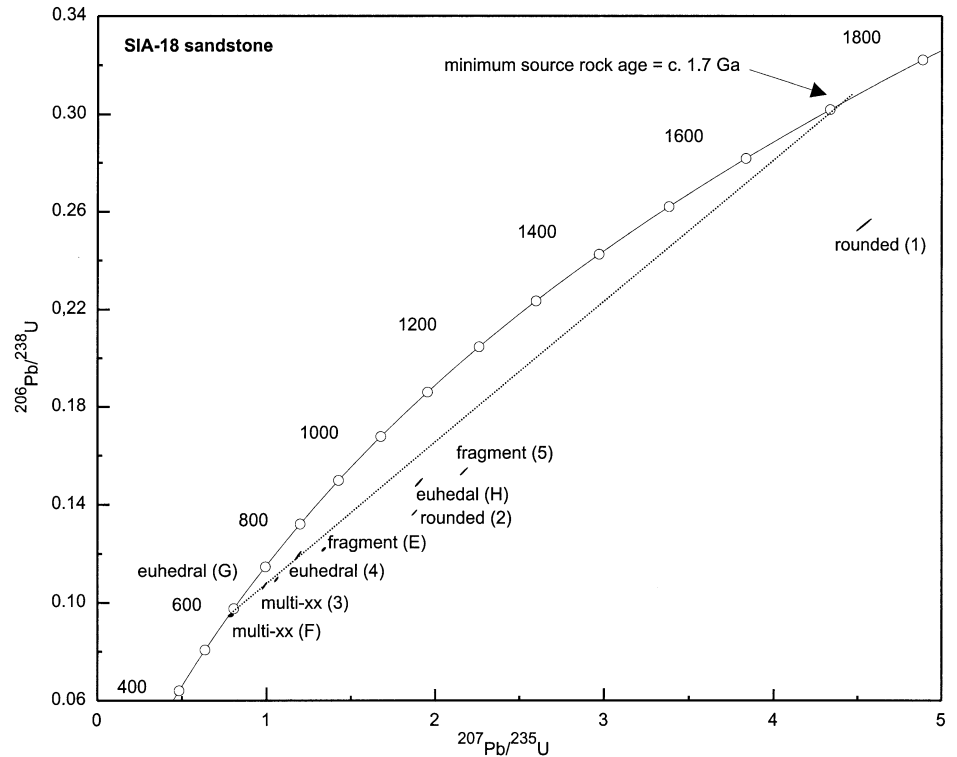


Fig. 6 U-Pb zircon concordia of the Upper Neoproterozoic SIA-18 sandstone sample. Added to the figure is a *discordia* drawn from 0.6 Ga (assumed time of episodic Pb loss) whose upper intercept constrains the minimum age for the source rocks supplying zircons to the sandstone



Discussion

The general geochemical features of the UN and LC rocks are contrasting and some chemical parameters and relationships can be used for discriminant purposes (e.g., Ti and Zr abundances; CIA values; ratios such as $\text{Al}_2\text{O}_3/\text{TiO}_2$, K/Rb, Ti/Nb, Rb/Zr, etc.). A second aspect is the remarkable geochemical homogeneity of the UN rocks, as is indicated by the restricted ranges of element contents and element ratios in the shales and sandstones and by the practically identical average values of ratios such as $\text{Al}_2\text{O}_3/\text{TiO}_2$, Ti/Nb, Eu/Eu*, (La/Yb)_n, (Gd/Yb)_n and Th/U in all of these rocks (see Table 1). These features suggest that the source materials for UN rocks participated in more than one sedimentary cycle. By contrast, the geochemical features of the LC rocks suggest a less mature, more heterogeneous and more fractionated source. Finally, from the geochemical results on the UN shales and sandstones it is apparent that mineral fractionation during sedimentary processes did not seriously affect these rocks. As indicated above, however, the geochemical features of the LC shales and sandstones suggest mineral alteration and Th, U, Zr and REE redistribution and fractionation. The sedimentary rocks showing these characteristics are from the LC units that received the contribution of uppermost Neoproterozoic sediments that were weathered and reworked during the relative sea fall at late Neoproterozoic–Early Cambrian times in the CIZ (Valladares et al. 2000). These results are consistent with previous evidence for HREE-enrichment and negative Ce anomalies found in the LC shales (Ugidos et al. 1999).

Comparison of available U-Pb zircon data from the Iberian Peninsula

The U-Pb zircon data obtained in this study tend to define fan-shaped patterns that are suggestive of multi-stage histories. Due to a pronounced data discordance, which for many of the analyses is as high as 70–95%, and assuming a Pb-loss event at 0.6 Ga (see below), straightforward interpretations are difficult to make. Discordant data suggest a post-crystallization history that involved either a secondary Pb-loss or a young overgrowth on previously formed zircons, or a combination of both processes. It is important to determine whether one or several Pb-loss events are likely to have occurred. In the simplest case, only a recent Pb-loss has influenced the U-Pb systematics and this implies that $^{207}\text{Pb}/^{206}\text{Pb}$ ages for residual zircons in a sediment are an approximately representation of the true provenance ages. A single-stage Pb loss that took place at some stage prior to recent time implies that $^{207}\text{Pb}/^{206}\text{Pb}$ ages are only minimum ages. A more complicated age data structure would appear if two Pb-loss events had affected the U-Pb zircon system, and the resulting data would then plot inside a triangle, the corners of which would touch the concordia at the times of the first Pb-loss event, the second Pb-loss event and the primary crystallization age, respectively. Given the possibility that several source rock (crystallization) ages also exist and that the exact ages of the hypothetical Pb-loss events are less well constrained, one would end up with a very complex data pattern that may not be solvable. However, there are two circumstances that help to constrain the possible interpretations of the zircon data.

Table 5 Synthesis of Sm-Nd isotopic data

	$\epsilon_{\text{Nd}}(545)$	T_{DM} (Ga)	Authors
Lower Cambrian	-7.3 to -7.2	1.6 to 1.7	Nägler et al. 1995
	-6.9	1.7 to 1.8	Beetsma 1995
	-7.0 to -3.8	1.5 to 1.8	Ugidos et al. 1997a, 2003
Upper Neoproterozoic	-5.8 to -2.8	1.5 to 1.7	Nägler et al. 1995
	-3.5 to -2.0	1.4 to 1.7	Beetsma 1995
	-3.7 to -1.7	1.3 to 1.4	Tassinari et al. 1996
	-3.5 to -0.4	1.1 to 1.8	Ugidos et al. 1997a, 2003

One is the availability of independent isotopic and geological data, and the second one is that there are certain tendencies for the present U-Pb zircon data to plot along discordias.

Before discussing the zircon data from this study in detail, it is appropriate to address the significance of other published isotopic and geochemical data from comparable rocks. It is of particular interest to discover whether other studies have provided information about geological events that led to Pb-losses in zircon, and also to compile the ages for source areas that have evidently supplied detritus to rocks of Iberia. It is clear from previous conventional, multi-grain zircon studies in Spain that the U-Pb data often are highly discordant. Despite this, it has been possible to interpret some important features, involving the main age intervals for potential source areas, and the mechanisms and time constraints for the inferred Pb-loss events. Exemplifying this are age-dating studies in which a Gondwana-provenance for Phanerozoic sediments in Iberia has been suggested (Schäfer et al. 1993; Kuijper et al. 1982). In these studies, it is argued that two main age populations dominate among the analyzed detrital zircons; one consistent with a Pan-African age span (age data dominantly between 0.7 and 0.6 Ga), and the other suggesting Early Proterozoic sources (mainly 2.2 to 1.8 Ga in age, with fewer Archean ages).

As mentioned previously, the inferred Pb-losses in zircons from Iberia are, a common feature that is sometimes coupled to new zircon growth. For instance, Pb-losses at 540, 380 and 300 Ma are indicated for Early Paleozoic gneisses in the Sierra de Guadarrama, Mirando do Douro and Viana del Bollo-Puebla de Sanabria areas (Wildberg et al. 1989; Lancelot et al. 1985), and the U-Pb data for zircons also suggest precursor ages, varying between 2.0 and 2.4 Ga. Still another Phanerozoic rock in NW Spain, interpreted as a paragneiss, yielded a similar discordant age data pattern, which was assumed to reflect a secondary Pb-loss of 2.0 Ga zircons as a response to a strong metamorphic event at 470 Ma (Kuijper et al. 1982). However, a concordant SHRIMP age of 480 Ma for gneisses has been reported by Valverde-Vaquero and Dunning (2000), illustrating the common observation that ion probe ages may be concordant while conventional ages for similar zircon populations are discordant.

It is evident that specific events have occasionally led to Pb-losses in the zircons now found in Phanerozoic successions within the CIZ. For the unmetamorphosed samples studied here, no metamorphic events of the type

mentioned above that have post-dated the deposition of the Upper Neoproterozoic–Lower Cambrian succession in the CIZ are relevant. However, Pb-losses may have occurred before the depositional stage in connection with metamorphism in the source area, or at a relatively late stage, in connection with transport, reworking during the sea level fall at around 0.54–0.55 Ga, and diagenesis processes in the sedimentation area. It is also possible that even later post-diagenetic geological events, the Hercynian (0.4–0.3 Ga) orogeny, and recent weathering and uplift processes connected with the Tertiary Alpine orogeny (cf. fission-track ages around 10 Ma for apatite; Sell et al. 1995) may have induced late-stage Pb-losses.

A critical examination of the U-Pb data obtained in light of other evidence

Table 5 offers a synthesis of Sm-Nd isotopic results on shales from different areas in the CIZ (e.g. Nägler et al. 1995; Beetsma 1995; Tassinari et al. 1996; Ugidos et al. 1997b, 2003), recalculated to 545 Ma. The ranges of ϵ_{Nd} values and T_{DM} model ages of the Neoproterozoic and Lower Cambrian fine-grained rocks partially overlap. Therefore, a distinction between two different source areas seems difficult or impossible. However, it must be taken into account that the extreme values of ϵ_{Nd} (e.g., those between -5.8 and -3.5 for Neoproterozoic) and T_{DM} model ages (e.g., 1.4 and 3.2 Ga for LC) correspond to samples of imprecise stratigraphic position and/or to samples that have $^{147}\text{Sm}/^{144}\text{Nd}$ ratios higher than 0.130. Such elevated ratios are probably related to REE redistribution and, consequently, do not correspond to primary values (e.g., Zhao et al. 1992). Some evidence for REE mobilization is given above and anomalous enrichments in Y (up to four times background content) and Ce negative anomalies ($\text{Ce}/\text{Ce}^*=0.65$ to 0.83) have been reported previously (Ugidos et al. 1999, 2003) for the LC shales. The sea-level fall and subsequent subaerial reworking of sediments commented above are the most probable cause for these geochemical anomalies. The Neoproterozoic rocks show ϵ_{Nd} values higher than -3.5 and T_{DM} model ages younger than 1.5 Ga if the anomalous samples are excluded. By contrast, the LC samples have ϵ_{Nd} values ranging from -7.3 to -4.4 and T_{DM} model ages ranging from 1.6 to 1.8 Ga. Given that these results separate the UN from LC rocks in different areas of the CIZ (see authors above), it seems logical to accept that such a distinctive feature is of general rather

than local significance, as would also be the case for the geochemical data. The Sm-Nd isotope results shown in Table 5 are similar to those for the Neoproterozoic and Lower Cambrian fine-grained sedimentary rocks (Nägler et al. 1995) from the Cantabrian Zone. That is, if Nd isotope data are compared on a larger scale, it is clear that similar Nd isotope patterns characterize not just the present study area, but the whole of the CIZ and also other zones in Spain. This kind of unifying feature strongly suggests that Gondwana was the general provenance area for the detrital rock components in these areas. An implication of this is that the U-Pb data patterns indicated for zircons from sediments elsewhere in Spain, showing a dual age distribution at 0.7–0.6 and 2.2–1.8 Ga, are also likely to be valid for rocks discussed here.

However, although Nd isotope data in general suggest a common provenance for the study area and the surrounding rock provinces, there are also Nd isotopic differences that distinguish sediments of Lower Cambrian and Upper Neoproterozoic age, respectively. Unfortunately, no Sm-Nd isotope data exist for the sandstones in the CIZ. It is known, however, that shales that are spatially associated with the Neoproterozoic sandstone SIA-18 have uniform neodymium model ages that are much younger (1.1 Ga) than the LC shales (1.6 Ga), (Ugidos et al. 2003). Therefore, it seems logical to assume that the Nd isotope differences separating shales of UN and LC origin should also characterize the corresponding sandstones. Apart from Nd isotopic differences, there are also distinct petrological and geochemical differences among the CIZ sediments (Ugidos et al. 1997a, 1997b; Valladares et al. 2000, 2002b). From this it follows that even though the sources for UN and LC siliciclastic rocks are both mature, they differ to some extent, and a recycled orogen and a craton interior, respectively, are indicated. Taking the Nd isotope and petrological/geochemical features together, it is clear that the individual sources for UN and LC sandstones must be different. In an age perspective, this suggests that the U-Pb isotope features for zircons should be different in the two rocks studied here, sandstone SIA-18 and sandstone SSA-5. Although the typical Gondwana age populations in the 0.7–0.6 and 1.8–2.2 Ga intervals are expected, the input of zircons from the respective age interval as well as the zircon types are expected to differ. It is thus unlikely that zircons analyzed in this study originated from source areas characterized by ages that fall significantly outside these intervals. In keeping with this reasoning is the fact that although rifting of the Gondwana-continent had already started at 0.9 Ga, this type of magmatism is not likely to generate many zircons.

The UN sandstone (SIA-18 sample) has a slightly more juvenile character as compared with the SSA-5 sample. This is consistent with the fact that the zircon morphology of this sample is more complex than what was noted for SSA-5, suggesting that the erosional processes connected with the sedimentation of SIA-18 involved detritus from an age-zoned provenance area. If we combine this observation with the low, relatively

speaking, Nd model ages for the UN sediments, a specific input of detritus from a young, juvenile source is indicated. Such a source could be of Pan-African age (0.7–0.6 Ga), which would suggest that zircons of this age interval should be present in the SIA-18 sample. The U-Pb data obtained actually support this, as illustrated by the near-concordant multi-faceted fraction F (Fig. 6). This fraction, showing a metamorphic habitus, yielded a $^{207}\text{Pb}/^{206}\text{Pb}$ age of 0.61 ± 0.3 Ga, which most likely reflects a growth of zircon linked to metamorphism. Such a metamorphic event is likely to have been responsible for significant Pb-losses in zircons of older provenance. In particular, zircons in mature sediments, like the ones studied here, would probably be prone to losing radiogenic lead. This is because the passage through several erosional cycles and related exposure to circulating solutions and changing Eh conditions would have probably made zircons more susceptible to losing Pb during later metamorphic events occurring during elevated temperatures.

If an age of 0.6 Ga is considered to be the formation age for the fraction F, it is logical that the other analyzed multi-faceted fraction, SIA-18(3), also formed at this time. However, this fraction shows an inheritance and apparently a discordia originating from 0.6 Ga (inferred time of Pb-loss) through this point would give an estimate of the age of the inferred older source. Due to the short distance between the points reflecting the 0.6 Ga age on the concordia and the analyzed Pb/U ratios for this fraction, respectively, this exercise will only yield a rough indication of a source age in the 2.0–2.2 Ga range. However, the age obtained in this way is typical for a Gondwana continental source.

Although they cannot be completely ruled out, there are no clear indications of any post-0.6 Ga events, and associated Pb-losses, that have affected the zircons in this sample. Supporting this is the concordant position of the multi-faceted type (F fraction), which at least indicates that no severe post-0.6 Ga event has affected this zircon type. It is true that the Rb-Sr isotopic system shows disturbances in shales of both the UN and LC successions in the CIZ (Beetsma 1995; Ugidos et al. 1997b), but it also is possible that such effects are small on rocks from lower UN strata, cf. SIA-18=unit I, not exposed to subaerial conditions in connection with the relative sea-level fall, and more pronounced further up in the stratigraphic succession. If no post-0.6 Ga events are assumed to have affected the U-Pb zircon system, then all discordant U-Pb zircon data for SIA-18 are basically due to a simple single-stage Pb-loss event at 0.6 Ga. In other words, the spread in the concordia diagram defined by the discordant data points could mainly be due to a variation in source rock ages, which could be estimated by drawing discordias, starting at the 0.6 Ga concordant position, through the individual data points in Fig. 6. The upper intercepts obtained in this way define a relatively narrow age span; that is, from 1.7 to 2.2 Ga. Since this age span fits known ages from the Gondwana continent, this

approach appears to be justified. It should also be recalled that certain core-mantle over-growths were observed in the SIA-18 sample, and it is logical that metamorphism at 0.6 Ga would have caused such over-growths on zircon relics of Gondwana provenance. However, this type of process would give the same effect in the age concordia diagram as an inferred Pb-loss, and would not essentially change the argument. We may thus conclude that the bimodal age populations obtained for the SIA-18 sample are in keeping with relatively low Nd model ages and consistent with, though not necessarily implying, a Gondwana continent origin for the detritus.

The SSA-5 sandstone of the LC succession was deposited around 540 Ma and contains zircon grains which are all small and show a limited morphological variability. Still, U-Pb isotope data are seemingly variable and appear to indicate several provenance ages. When discussing the zircon types observed in the SIA-18 and SSA-5 samples, one must not only consider that differences should exist because of distinct provenance areas, but also acknowledge that re-processing of the uppermost UN sediments during the sea-level fall is likely to have contributed to the SSA-5 sandstone sample. Considering that Nd isotope signatures are consistent within the successions made up by LC and UN sediments, respectively, it can be anticipated that zircon morphologies are similar within a succession, and different when the two different successions are compared. Thus, as a first approximation, zircon types representative of SIA-18 (unit I) could have been contributing to the SSA-5 (unit VII) even if the sea level fall only affected units IV and III in the UN succession. Thus, SSA-5 should carry zircons typical of its provenance area and, also, additional zircons may have been added in connection with reworking of the upper parts of the UN succession. When checking the zircon types found in the SSA-5, the multi-faceted type (F and 3) and the well-rounded type (1 and 2) typical of SIA-18 were not observed. The fact that these zircon morphologies are missing in SSA-5 may be due to some kind of fractionation process, the existence of which is indicated from geochemical data. The details of the hydrodynamic conditions prevailing during reworking are difficult to determine, and possibly some Upper Proterozoic zircons became selectively added to the SSA-5 but apparently not the euhedral or the rounded type. The rather uniform morphology appears to indicate that SSA-5 zircons were predominantly supplied from a single, distant source area, rather than being due to a local reworking process, considering also that in general only a few zircons were present in the sample.

According to the relatively old Nd model ages for the LC rocks, and given the above assumption that the zircons in the SSA-5 should basically reflect the ultimate provenance area, a dominance of old zircons is expected. The pronounced discordance again obstructs clear-cut conclusions, but the visual impression is that the obtained U-Pb data on zircon do not obviously support this view. Only fraction A (angular fragments) really requires an old Proterozoic origin. Its $^{207}\text{Pb}/^{206}\text{Pb}$ age is 1.47 Ga, which is

an age that falls outside any age interval known to characterize a Gondwana source, and consequently a post-crystallization Pb-loss has most likely affected these zircons. Similarly to the argumentation for the SIA-18 sample, the strong discordance may be due to a significant Pb-loss at 0.6 Ga. Thus, fraction A zircons formed at 1.8 Ga if the assumption of a secondary lead loss at 0.6 Ga is valid. The remaining three zircon fractions from this sample have relatively low $^{207}\text{Pb}/^{206}\text{Pb}$ ages and are not easily reconciled with an old provenance coupled to a 0.6 Ga Pb-loss. An old provenance would require an extreme Pb-loss, and in part the high U content encountered for fractions B and D could have induced very significant Pb-losses as a result of metamictization. A speculative explanation would be that all zircon fractions in SSA-5 would have derived from an old source comprising lithologies of a limited age span. Subsequently, zircons underwent multi-stage Pb-loss behaviour and were affected by at least one process subsequent to an inferred 0.6 Ga Pb-loss event, which led to variable Pb-losses. Supporting this theory is the established reworking process at around 540 Ma that did affect the detrital components of the SSA-5 sample and which may have led to an effect on the U-Pb systematics of the zircons. In the case of a multi-stage Pb loss, or a more continuous type of Pb loss, involving a very strong 0.6 Ga Pb-loss and another event at around 540 Ma that also induced a Pb loss, the U-Pb data for the C and D fractions could tentatively occupy similar positions in the concordia diagram as those observed by assuming that almost all radiogenic Pb was lost during processes in the 0.60–0.54 Ga interval. However, in order to explain the position of fraction B, an even younger event, or a more continuous radiogenic Pb loss, is required. This fraction plots similarly to the data from Upper Precambrian-Ordovician ortho-gneisses in NW Iberia (Lancelot et al. 1985) which were ascribed to a process involving a continuous Pb loss. Apparently, there is no compelling isotopic evidence to suggest that SSA-5 zircons did originate to a significant degree from an old cratonic source (cf. geochemical modelling), but the anticipated history of this rock unit allows that this could be the case.

Concluding remarks

On the basis of geochemical features, the UN sandstones and shales can be discriminated from the equivalent LC rocks in the CIZ. In general terms, the former have relatively restricted ranges of element abundances and ratios, are less fractionated and are chemically more mature than the other ones. Their homogeneity is also remarkable since the average values of some parameters [e.g. $\text{Al}_2\text{O}_3/\text{TiO}_2$, Ti/Nb, Eu/Eu^* , $(\text{La}/\text{Yb})_n$, $(\text{Gd}/\text{Yb})_n$ and Th/U] are practically the same for both the sandstones and shales. These features strongly support the notion that mineral fractionation did not affect the detrital materials during sedimentary processes and suggest a homogeneous and recycled source area for the UN siliciclastic rocks. By

contrast, the LC rocks are less mature and more heterogeneous, as indicated by their lower CIA values and broader ranges of element abundances and element ratios. Also, the lower Eu/Eu* and higher (La/Yb)_n and Th/Yb ratios suggest a relatively more fractionated source area. The Ti and Zr abundances, CIA values, and element ratios such as Al₂O₃/TiO₂, K/Rb, Ti/Nb, Rb/Zr, can be used for discriminating purposes between the UN and LC siliciclastic rocks.

The conventional U-Pb isotope technique applied to zircons from two sandstones has given results that are not straightforward to interpret. Due to the observed high degree of discordance, several interpretations of the ages and post-crystallization histories are possible. However, differences in grain size, zircon morphology, and the principal arrangement of U-Pb data are noteworthy for the studied zircons in the two rocks. On the basis of these features, and the distinct geochemical and Sm-Nd isotopic differences between the rocks investigated, it is argued that the zircon populations of the two sandstones must have originated from different source areas. Upon comparison with petrological and isotopic data obtained from other sedimentary areas in the CIZ and elsewhere in Iberia, we favour a Gondwana (West Africa craton) provenance for the sediments in the CIZ. Further isotopic zircon work involving single-grain studies is necessary to reach a deeper understanding.

Acknowledgements Financial support for this work was provided by the PB91-0321 DGICYT project, the PB96-1283 DGES project, and the BTE 2002-04241-CO2-02 of the MEC (Spain). This paper is a contribution to the International Geological Correlation Programme Project 453 "Ancient and Recent Orogens". Comments by two anonymous reviewers led to improvements in the paper.

References

- Beetsma JJ (1995) The late Proterozoic/Paleozoic and Hercynian crustal evolution of the Iberian Massif, N Portugal: as traced by geochemistry and Sr-Nd-Pb isotope systematics of pre-Hercynian terrigenous sediments and Hercynian granitoids. Doctoral Diss, Vrije Univ, Amsterdam, 223 pp
- Black R, Liegeois J-P (1993) Cratons, mobile belts, alkaline rocks and continental lithospheric mantle: the Pan-African testimony. *J Geol Soc Lond* 150:89-98
- Black R, Latouche L, Liegeois J-P, Caby R, Bertrand JM (1994) Pan-African displaced terranes in the Tuareg shield (central Sahara). *Geology* 22:641-644
- Bock B, McLennan SM, Hanson GN (1994) Rare earth element redistribution and its effects on the neodymium isotope system in the Austin Glen Member of the Normanskill Formation, New York, U.S.A. *Geochim Cosmochim Acta* 58:5245-5253
- Cotten J, Le Dez A, Bau M, Caroff M, Maury RC, Dulsky P, Fourcade S, Bohn M, Brousse R (1995) Origin of anomalous rare-earth element and yttrium enrichments in subaerially exposed basalts: evidence from French Polynesia. *Chem Geol* 119:115-138
- Cullers RL (1995) The controls on the major- and trace-element evolution of shales, siltstones and sandstones of Ordovician to Tertiary age in the West Mountains region, Colorado, U.S.A. *Chem Geol* 123:107-131
- Dabard MP, Loi A, Peucat JJ (1996) Zircon typology combined with Sm-Nd whole-rock isotope analysis to study Brioverian sediments from the Armorican Massif. *Sediment Geol* 101:243-260
- Dickinson WR, Beard LS, Brakenridge GR, Erjavec JL, Ferguson RC, Inman KF, Knepp RA, Lindberg FA, Ryberg PT (1983) Provenance of North American Phanerozoic sandstones in relation to tectonic setting. *Geol Soc Am Bull* 94:222-235
- Díez Balda MA, Vegas R, González Lodeiro F (1990) Central Iberian Zone (Autochthonous Sequences). Structure. In: Dallmeyer RD, Martínez García E (eds) *Pre-Mesozoic geology of Iberia*. Springer, Berlin Heidelberg New York, pp 172-188
- Fernández-Suárez J, Gutiérrez-Alonso G, Jenner GA, Tubrett MN (2000) New ideas on the Proterozoic-Early Paleozoic evolution of NW Iberia: insights from U-Pb detrital zircon ages. *Precambrian Res* 102:185-206
- Goodwin AM (1991) *Precambrian geology*. Academic Press, London, pp 1-666
- Guerrot C, Peucat JJ, Capdevila R (1989) Archean protoliths within Early Proterozoic granulitic crust of the west European Hercynian belt: possible relics of the west Africa craton. *Geology* 17:241-244
- Guerrot C, Calverz JY, Bonjour JL, Chantraine J, Chauvel JJ, Dupret L, Rabu D (1992) Age du Briovérien de Bretagne centrale et occidentale: contraintes radiométriques. *C R Acad Sci Paris* 315:1741-1746
- Hébert R (1995) Evidence for multiple high-T metamorphism and regional migmatization within the Cadomian belt of northern Brittany, France. *J Geol Soc Lond* 152:213-216
- Kemnitz H, Romer RL, Oncken O (2002) Gondwana break-up and the northern margin of the Saxothuringian belt (Variscides of central Europe). *Int J Earth Sci* 91:246-259
- Krogh TE (1973) A low-contamination method for hydrothermal decomposition of zircon and extraction of U and Pb for isotopic age determination. *Geochim Cosmochim Acta* 37:485-494
- Kuijper RP, Priem HNA, Den Tex E (1982) Late Archean-early Proterozoic sources of ages of zircons in rocks from the Paleozoic orogen of western Galicia, NW Spain. *Precambrian Res* 19:1-29
- Lancelot JR, Allegret A, Iglesias Ponce de León M (1985) Outline of Upper Precambrian and Lower Paleozoic evolution of the Iberian Peninsula according to U-Pb dating of zircons. *Earth Planet Sci Lett* 74:325-337
- Linnemann U, Romer RL (2002) The Cadomian orogeny in Saxo-Thuringia, Germany: geochemical and Nd-Sr-Pb isotopic characterization of marginal basins with constraints to tectonic setting and provenance. *Tectonophysics* 352:33-64
- Ludwig K (2001) ISOPLOT/Ex version 2.49. A geochronological toolkit for Microsoft Excel. Berkeley Geochronology Center Spec Pub 1A, pp 1-56
- McLennan SM (1989) Rare earth elements in sedimentary rocks: influence of provenance and sedimentary processes. In: Lipin BR, McKay GA (eds) *Geochemistry and mineralogy of rare earth elements*. *Rev Mineral* 21:169-200
- Nägler TF, Schäfer HJ, Gebauer D (1995) Evolution of the Western European continental crust: implications from Nd and Pb isotopes in Iberian sediments. *Chem Geol* 121:345-357
- Nance RD, Murphy JB (1994) Contrasting basement isotopic signatures and palinspastic restoration of peripheral orogens: example from the Neoproterozoic Avalonian-Cadomian belt. *Geology* 22:617-620
- Nesbitt HW (1979) Mobility and fractionation of rare earth elements during weathering of a granodiorite. *Nature* 279:206-210
- Nesbitt HW, Markovicks G (1997) Weathering of granodioritic crust, long-term storage of elements in weathering profiles, and petrogenesis of siliciclastic sediments. *Geochim Cosmochim Acta* 61:1653-1670
- Nesbitt HW, Wilson RE (1992) Recent chemical weathering of basalts. *Am J Sci* 292:740-777
- Nesbitt HW, Young GM (1982) Early Proterozoic climates and plate motions inferred from major element chemistry of lutites. *Nature* 299:715-717

- Öhlander B, Ingri J, Land M, Schöberg H (2000) Change of Sm-Nd isotope composition during weathering of till. *Geochim Cosmochim Acta* 64:813–820
- Pin C (1991) Central-western Europe: major stages of development during Precambrian and Paleozoic times. In: Dallmeyer RD, Lécorché JP (eds) *The West African orogens and Circum-Atlantic correlatives*. Springer, Berlin Heidelberg New York, pp 295–306
- Pin C, Liñán E, Pascual E, Donaire T, Valenzuela A (1999) Late Proterozoic crustal growth in Ossa Morena: Nd isotope and trace element evidence from the Sierra de Córdoba volcanics. *J Conf Abstr* 4:1019
- Quesada C, Apalategui O, Eguíluz L, Liñán E, Palacios T (1990) Ossa-Morena Zone. 2. Stratigraphy. Precambrian. In: Dallmeyer RD, Martínez García E (eds) *Pre-Mesozoic geology of Iberia*. Springer, Berlin Heidelberg New York, pp 252–258
- Schäfer HJ, Gebauer D, Nägler TF, Eguíluz L (1993) Conventional and ion-microprobe U-Pb dating of detrital zircons of the Tentudía Group (Serie Negra, SW Spain): implications for zircons systematics, stratigraphy, tectonics and Precambrian/Cambrian boundary. *Contrib Mineral Petrol* 113:289–299
- Sell I, Poupeau G, Casquet C, Galindo C, González Casado JM (1995) Exhumación Alpina del bloque morfotectónico Pedriza-La Cabrera (Sierra del Guadarrama, Sistema Central Español): potencialidad de la termocronometría por trazas de fisión en apatitos. *Geogaceta* 18:23–26
- Simien F, Mattauer M, Allègre CJ (1999) Nd isotopes in the stratigraphic record of the Montagne Noire (French Massif Central): no significant Paleozoic juvenile inputs, and pre-Hercynian paleogeography. *J Geol* 107:87–97
- Tassinari CCG, Medina J, Pinto MS (1996) Rb-Sr and Sm-Nd geochronology and isotope geochemistry of Central Iberian metasedimentary rocks (Portugal). *Geol Mijnbouw* 75:69–79
- Taylor SR, McLennan SM (1985) *The continental crust: its composition and evolution*. Blackwell, London, pp 1–312
- Tichomirowa M, Bertger H-J, Koch EA, Belyatski BV, Götze J, Kempf U, Nasdala L, Schaltegger U (2001) Zircon ages of high-grade gneisses in the eastern Erzgebirge (central European Variscides)-constraints on origin of the rocks and Precambrian to Ordovician magmatic events in the Variscan fold belt. *Lithos* 56:303–332
- Ugidos JM, Valladares MI, Barba P, Ellam RM (2003) The Upper Neoproterozoic-Lower Cambrian of the Central Iberian Zone, Spain: chemical and isotopic (Sm-Nd) evidence that the sedimentary succession records an inverted stratigraphy of its source. *Geochim Cosmochim Acta* 67:2615–2629
- Ugidos JM, Armenteros I, Barba P, Valladares MI, Colmenero JR (1997a) Geochemistry and petrology of recycled orogen-derived sediments: a case study from the Upper Precambrian siliciclastic rocks of the Central Iberian Zone, Iberian Massif, Spain. *Precambrian Res* 84:163–180
- Ugidos JM, Valladares MI, Barba P, Armenteros I, Colmenero JR (1999) Geochemistry and Sm-Nd isotope systematics on the Upper Precambrian-Lower Cambrian sedimentary successions in the Central Iberian Zone, Spain. *J Conf Abstr* 4:1021
- Ugidos JM, Valladares MI, Recio C, Rogers G, Fallick AE, Stephens WE (1997b) Provenance of Upper Precambrian/Lower Cambrian shales in the Central Iberian Zone, Spain: evidence from a chemical and isotopic study. *Chem Geol* 136:55–70
- Valladares MI, Barba P, Ugidos JM (2002a) Precambrian. In: Gibbons W, Moreno T (eds) *Geology of Spain*. Geol Soc Lond Spec Pub, London, pp 7–16
- Valladares MI, Ugidos JM, Recio C (1993) Criterios geoquímicos de correlación y posible área fuente de las pelitas del Precámbrico Superior-Cámbrico Inferior de la Zona Centro Ibérica (Macizo Ibérico, España). *Rev Soc Geol Esp* 6:37–45
- Valladares MI, Ugidos JM, Barba P, Colmenero JR (2002b) Contrasting geochemical features of the Central Iberian Zone shales (Iberian Massif, Spain): implications for the evolution of Neoproterozoic-Lower Cambrian sediments and their sources in other Peri-Gondwanan areas. *Tectonophysics* 352:121–132
- Valladares MI, Barba P, Colmenero JR, Armenteros I, Ugidos JM (1998) La sucesión sedimentaria del Precámbrico Superior-Cámbrico Inferior en el sector central de la Zona Centro Ibérica: Litoestratigrafía, geoquímica y facies sedimentarias. *Rev Soc Geol Esp* 1:271–283
- Valladares MI, Barba P, Ugidos JM, Colmenero JR, Armenteros I (2000) Upper Neoproterozoic-Lower Cambrian sedimentary successions in the Central Iberian Zone (Spain): sequence stratigraphy, petrology and chemostratigraphy. Implications for other European areas. *Int J Earth Sci* 89:2–20
- Valverde-Vaquero P, Dunning GR (2000) New U-Pb ages for Early Ordovician magmatism in central Spain. *J Geol Soc Lond* 157:15–26
- Valverde-Vaquero P, Dörr W, Belka Z, Franke W, Wiszniewska J, Schastok J (2000) U-Pb single-grain dating of detrital zircon in the Cambrian of central Poland: implications for Gondwana versus Baltica provenance studies. *Earth Planet Sci Lett* 184:225–240
- Villeneuve M, Cornée JJ (1994) Structure, evolution and palaeogeography of the West African craton and bordering belts during the Neoproterozoic. *Precambrian Res* 69:307–326
- Wildberg HGH, Bischoff L, Baumann A (1989) U-Pb ages of zircons from meta-igneous and meta-sedimentary rocks of Sierra de Guadarrama: implications for the Central Iberian crustal evolution. *Contrib Mineral Petrol* 103:253–262
- Zeh A, Brätz H, Millar IL, Williams IS (2001) A combined zircon SHRIMP and Sm-Nd isotope study of high-grade paragneisses from the Mid-German Crystalline Rise: evidence for northern Gondwanan and Grenvillian provenance. *J Geol Soc Lond* 158:983–994
- Zhao JX, McCulloch MT, Bennett VC (1992) Sm-Nd and U-Pb zircon isotopic constraints on the provenance of sediments from the Amadeus Basin, central Australia: evidence for REE fractionation. *Geochim Cosmochim Acta* 56:921–940